Journal of Optoelectronics and Advanced Materials Vol. 5, No. 2, June 2003, p. 409 - 414

SUBSTRATE AND OXYGEN-ANNEALING EFFECTS ON THE PULSED-LASER-DEPOSITED $La_{0.5}Ca_{0.5}Mn_{1-x}M_xO_3$ (M = Fe, Ni) THIN FILMS

L. S. Hsu, C. J. Liu, T. W. Wu, D. Luca[a*]

Department of Physics, National Chang-Hua University of Education, Chang-Hua 50058, Taiwan, Republic of China

Perovskite manganite thin films of $La_{0.5}Ca_{0.5}MnO_3$ doped with 5% Fe or Ni were grown on $SrTiO_3$, $LaAlO_3$, and $NdGaO_3$ single-crystal substrates by pulsed-laser deposition. The as-deposited films were amorphous and epitaxial layers were obtained only after ex-situ post-annealing at 900 ^oC under 1 atmosphere of oxygen. The effects of different substrates and oxygen-annealing conditions of the films correlate with their structural, magnetoresistance, and electronic properties.

(Received April 17, 2003; accepted May 8, 2003)

Keywords: Perovskite, Pulsed-laser deposition, Magnetoresistance, X-ray absorption spectroscopy

1. Introduction

Perovskite-like $La_{1-x}A_xMnO_3$ (A = Ca, Sr, Ba, and Pb) materials are of special interest because they exhibit colossal magnetoresistance, where the electrical resistance of the materials changes by more than an order of magnitude under an applied magnetic field [1-3]. Much effort has been focused on the epitaxial growth of $La_{0.7}Ca_{0.3}MnO_3$ (LCMO) thin films for potential device applications [3,4]. It was reported [5] that the metal-insulator transition temperature of post-annealed LCMO films under O_2 at 900 °C decreases by more than 100 K compared with that of the as-grown films. The oxygen-annealed films also show thermal hysteresis in electrical resistivity [5]. These results were interpreted in terms of Mn deficiency induced by large structural difference between the laser-ablated films and the MgO (100) substrate. Recently, it has been proved that annealing or applying hydrostatic pressure on bulk $La_{1.4}Sr_{1.6}Mn_2O_7$ ceramics samples results in the same behaviors of the electrical resistivity and thermopower [6]. Moreover, the ferromagnetic cluster behaviors have been observed in bulk perovskites $La_{0.8}Sr_{0.2}Mn_{0.8}Ni_{0.2}O_3$ and $La_{0.7}Ca_{0.3}Mn_{0.8}Ni_{0.2}O_3$ [7]. A low-temperature magnetoresistance (MR) ratio as high as 60 % was also found in $La_{0.7}Ca_{0.3}Mn_{0.8}Ni_{0.2}O_3$, which was attributed to the spin-dependent scattering inside the grains.

Pulsed laser deposition (PLD) is known to be an excellent method for growing perovskite films [8-10]. It has also been shown that high-quality LCMO films can be grown on single-crystal substrates by the PLD technique [1]. The LCMO films are usually grown at a relatively high substrate temperature (> 700 ^oC) followed by annealing at a higher temperature of 900 ^oC in oxygen ambient [1, 11]. The MR ratio of > 80 % under a high magnetic field (> 6 T) has been reported [2, 3, 12]. In this work, the deposition of perovskite LCMO thin films doped with 5 % iron or nickel by PLD is reported, and the effects of different substrates and post-annealing on the properties of these manganite thin films are investigated.

[a] On leave from the Faculty of Physics, Al. I. Cuza University, Iasi, Romania
[*] Corresponding author: dluca@cc.ncue.edu.tw

2. Experimental

Three LCMO targets of nominal compositions ($La_{0.5}Ca_{0.5}MnO_3$, $La_{0.5}Ca_{0.5}Mn_{0.95}Ni_{0.05}O_3$, and $La_{0.5}Ca_{0.5}Mn_{0.95}Fe_{0.05}O_3$) were made by a standard solid-state reaction process. The targets were synthesized by quantitatively mixing high-purity powders of La_2O_3, $CaCO_3$, Mn_2O_3, and Fe_2O_3 or NiO. The detailed procedures for the preparation and characterization of these bulk samples are similar to those previously reported for $La_{1.4}Sr_{1.6}Mn_2O_7$ and $La_{0.67}Ca_{0.33}MnO_3$ ceramics [6,13]. Briefly, the mixed powders were calcined at 1300 °C in oxygen for 36 h with intermediate grinding. The resulting powders were then pressed into circular pellets of 1-cm diameter and 0.5-cm thickness and sintered at a temperature of 1300 °C for 18 h in air. X-ray diffraction (XRD) measurements on bulk samples showed standard LCMO peaks. The resistivity and thermopower measurements were also performed on bulk samples [13]. The oxygen contents and valence-state of the manganese were determined by iodometric titration [6,14].

Before the PLD deposition, the chamber was pumped down to a base pressure of 1×10^{-5} Torr.

During the PLD processes, a KrF excimer laser (λ = 248 nm) operating at a frequency of 10 Hz was focused on the surface of the target by a fused silica lens. The laser fluence on the surface of the target was estimated at about 1.5 J/cm^2. The films were grown on (100) $SrTiO_3$ (STO), (100) $LaAlO_3$ (LAO), and (100) $NdGaO_3$ (NGO) single-crystal substrates at a substrate temperature of 550 ^oC and oxygen pressure of 250 mTorr. These substrates are chosen to provide a range of lattice constants, which allows studies of the effects of tensile and compressive stress of the LCMO films. The substrate to target distance was kept 5 cm. A total number of 6000 laser shots were used to deposit each sample. *Ex-situ* post-annealing was performed on some samples at 900 ^oC in 1 atm of oxygen for 3 h.

The resistivity was measured using the four-point probe technique or the constant-voltage method depending on the resistance of the films. The applied field was parallel to the film surface and to the current flow direction. Depth profiles of elemental distribution in the films were measured with a Cameca IMS-4F secondary ion mass spectrometer (SIMS) using O_2^+ primary beam of 8 keV impact energy and 230 nA primary current. Only positive secondary ions were acquired. The structural properties of the as-deposited and post-annealed films were characterized by XRD using a Fe Kα (λ = 1.93604 Å) radiation.

3. Results and discussion

The thickness of the six LCMO films is determined to be within the 100-200 nm range from the SIMS measurements, as shown in Fig. 1. The SIMS spectra indicate that considerable amounts of Ni or Fe atoms are incorporated in the films, as can be seen from the similarity of their depth profiles. However, the oxygen content appears to be low. We also note that the oxygen signal decreases by two orders of magnitude for the LCMO films on the NGO substrate, while it decreases and increases within an order of magnitude for films on the LAO and STO substrates, respectively.

Fig. 2 shows the XRD patterns of the Ni- and Fe-doped LCMO films deposited on STO substrate at 550 ^oC and those subsequently post-annealed at 900 ^oC. The as-deposited films are amorphous as indicated by the absence of the LCMO XRD peaks and the presence of only the STO XRD peaks. The amorphous nature of the as-deposited films is due to the low growth temperature of 550 ^oC. However, annealing the films at 900 ^oC in 1 atmosphere of oxygen results in good crystalline structure of the LCMO films, whose peaks appear side by side with those of STO. Only LCMO (001) XRD reflections were observed. This observation confirms the highly textured growth of the LCMO films on the STO substrate. Similar observations are made on the LCMO films deposited on the LAO and NGO substrates.

We note that the lattice mismatches of LCMO on (100) LAO, STO and NGO substrates are –2.4, +0.6, and +0.1 %, respectively. Melting of charge ordering is evidenced by the fact that both Ni- and Fe-doped LCMO films undergo an insulator-metal transition at a temperature of 208 and 86.5 K, respectively. The transition shifts to a higher temperature of 216 K for Ni-doped and 87.4 K for doped LCMO films after applying a magnetic field of 5000 G.

As shown in Fig. 3, the $La_{0.5}Ca_{0.5}MnO_3$ film exhibits an insulating temperature dependence of resistivity and a charge ordering transition of roughly 125 K. However, virtually no thermal hysteresis is observed. For bulk $La_{0.5}Ca_{0.5}MnO_3$, the hysteresis behavior in resistivity is ascribed to the incommensurate-to-commensurate charge-ordering transition [15].

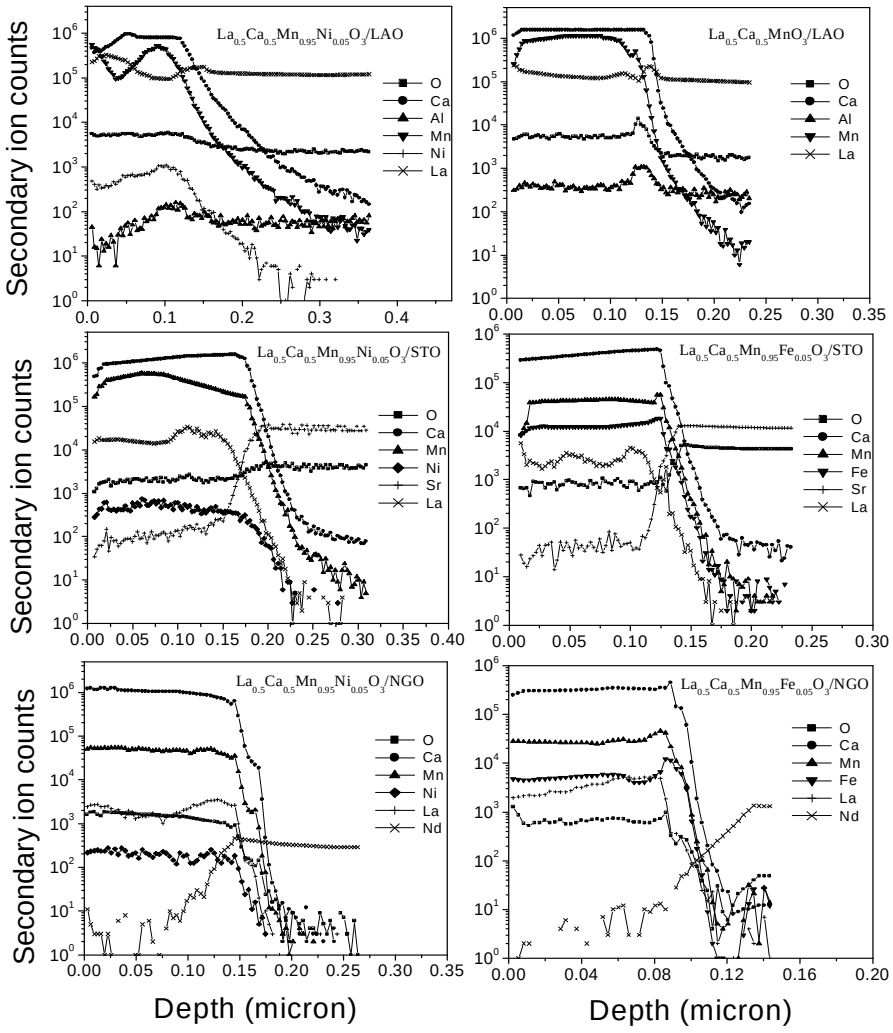

Fig. 1. SIMS spectra of the annealed Ni- and Fe-doped LCMO films.

It has been suggested that strong pinning by impurities and/or defects might result in residual discommensurations, which are often seen in the incommensurate phase as domain walls separating the small commensurate domains [15]. Therefore, the absence of thermal hysteresis in resistivity might indicate weak pinning or no impurity/defects in our $La_{0.5}Ca_{0.5}MnO_3$ film. In the same figure, the temperature dependence of resistivity for the Ni- and Fe-doped LCMO thin films deposited on the NGO substrate is shown.

The insulator-metal transition in the Ni-doped LCMO thin film is indicative of melting of charge ordering, whereas Fe-doped LCMO film retains the insulating behavior. These results are consistent with those found in bulk $La_{0.5}Ca_{0.5}Mn_{0.95}Ni_{0.05}O_3$ and $La_{0.5}Ca_{0.5}Mn_{0.95}Fe_{0.05}O_3$ in terms of temperature dependence of resistivity [14]. It has been suggested that smaller one-electron bandwidth W could stabilize the charge-ordered state due to larger interatomic Coulomb interaction [16-18]. It therefore implies that replacement of Mn site by Fe in LCMO would result in a smaller bandwidth W than that by the same doping level of Ni.

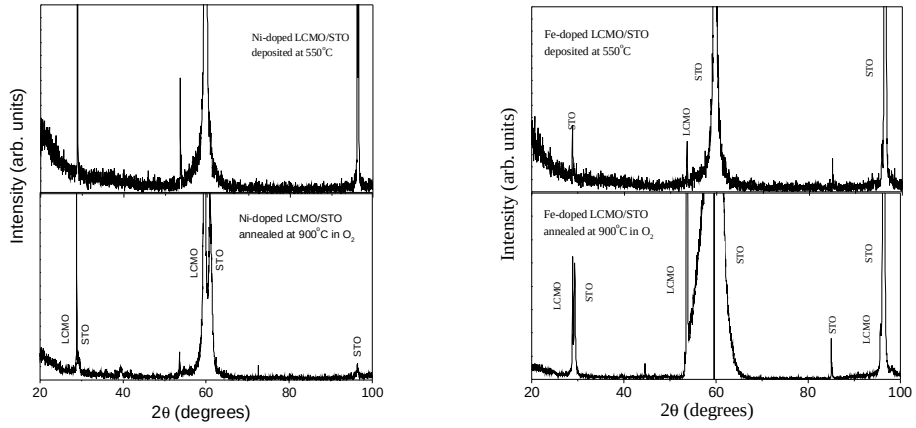

(a) (b)

Fig. 2. (a) XRD spectra of the as-deposited (550 °C) and post-deposition annealed (900 °C) Ni-doped LCMO films deposited on the STO substrate; (b) XRD spectra of the as-deposited (550 °C) and post-deposition annealed (900 °C) Fe-doped LCMO films deposited on the STO substrate.

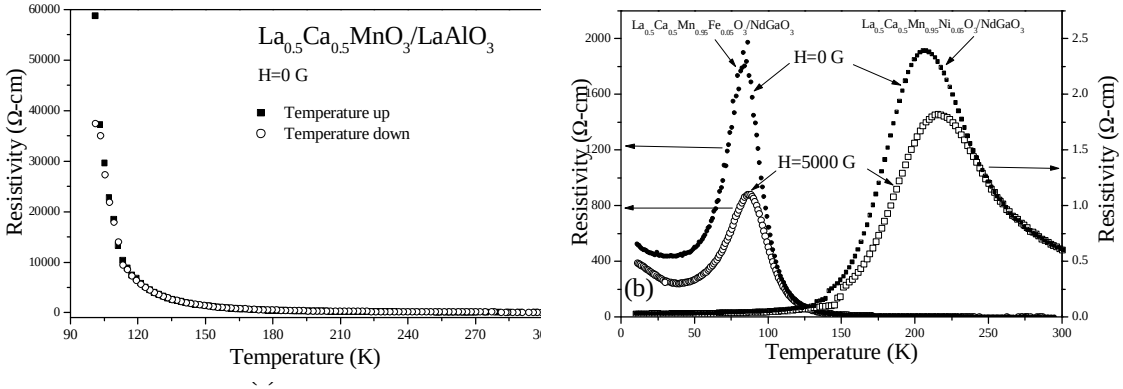

(a) (b)

Fig. 3. (a) The temperature dependence of resistivity upon cooling and warming for the post deposition annealed (900 °C) undoped LCMO thin films deposited on LAO substrates; (b) the temperature dependence of resistivity for the post deposition annealed (900 °C) Ni- and Fe - doped LCMO thin films deposited on the NGO substrates.

Table 1 shows the resistivity of the LCMO films measured at room temperature with and without an applied field. The resistivity varies from 0.05 to 2 Ω cm. Also shown in Table 1 are the MR ratios, defined as $(\rho_0-\rho_H)/\rho_0$, where ρ_0 and ρ_H are the resistivity measured with and without an applied magnetic field (7800 G) of the LCMO films measured at room temperature. The Ni-doped LCMO film exhibits a MR ratio of 39 % at 180 K at H = 5000 G.

Table 1. Resistivities measured with (ρ_H) and without (ρ_0) an applied magnetic field of 7800 G of the undoped, Ni- and Fe-doped LCMO thin films on various substrates.

Samples	ρ_0 (Ω cm)	ρ_H (Ω cm)	MR ratio (%)
$La_{0.5}Ca_{0.5}MnO_3/LaAlO_3$	0.054	0.050	7.4
$La_{0.5}Ca_{0.5}Mn_{0.95}Ni_{0.05}O_3/SrTiO_3$	1.960	1.840	6.1
$La_{0.5}Ca_{0.5}Mn_{0.95}Ni_{0.05}O_3/NdGaO_3$	0.220	0.210	4.5
$La_{0.5}Ca_{0.5}Mn_{0.95}Fe_{0.05}O_3/NdGaO_3$	0.280	0.240	14.3

The electronic structure of the LCMO thin films was examined by x-ray absorption spectroscopy (XAS) at beam lines 12A and 15B at the National Synchrotron Radiation Research Center (NSRRC), Taiwan. The XAS spectra were collected by recording the total yield of secondary electrons from the sample surfaces at room temperature. Figs. 4(a) and 4(b) display the x-ray absorption near-edge spectroscopy (XANES) spectra of the O K-edge and Mn $L_{2,3}$-edge, respectively, of the Fe- and Ni-doped LCMO films deposited on the NGO substrate.

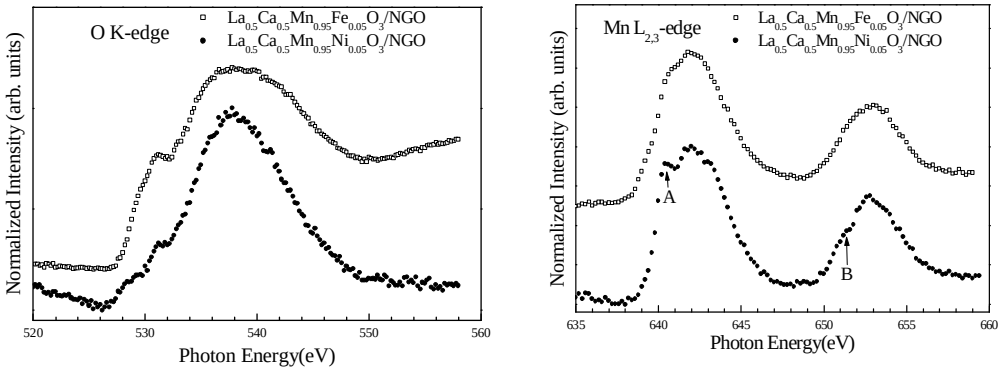

(a) (b)

Fig. 4. The normalized O K-edge (a) and Fe K-edge (b) x-ray absorption spectra of the post-deposition annealed (900 ^oC) undoped, Ni- and Fe-doped LCMO films deposited on the LAO and STO substrates.

In Fig. 4(a), the pre-edge structure (~530 eV) is associated to the transition into empty O 2p states hybridized with Mn 3d bands. The broad peak at 537 eV is attributed to O 2p states hybridized with La 5d states. Fig. 4(b) shows two spin-orbit split broad multiplet structures at 642 (L_3) and 652.8 eV (L_2). The broad features are associated to the more covalent character and the lower symmetry of the Mn ions in LCMO. There are also two crystal-field split shoulders (with crystal field splitting energy of 1.5 eV), indicated by A and B, on the low-energy side of the L_3 and L_2 regions, respectively.

Fig. 5 compares the Fe K near-edge XANES spectra of the 5 % Fe-doped LCMO film on STO and NGO substrates and that of a 5-μm Fe foil. The inflection point is at 7111.5 eV. One can readily see that the near-edge absorption spectrum is sharper and possesses more structures for the Fe-doped LCMO films than for the Fe metal. An increase of the Fe K near-edge intensity for the LCMO film corresponds to the increase of the number of empty Fe 4p-derived states. This result implies a decrease of the number of occupied Fe 4p-derived states and a loss of Fe 4p-orbital charge. Differences in the Fe K-edge XANES spectra were also noted for the two LCMO films on different substrates.

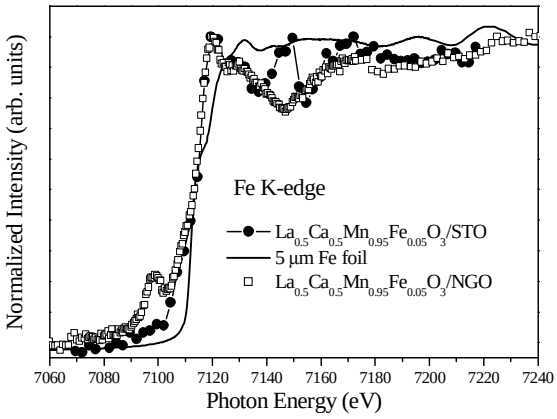

Fig. 5. The Fe K-edge XANES spectra of the 5 % Fe-doped LCMO films on the STO and NGO substrates and that of a 5 μm Fe foil.

The XAS and transport properties of the investigated films can be explained in terms of the effects of the interaction between pairs of Mn^{4+} and Mn^{3+}, which is responsible for both ferromagnetism and metal-nonmetal transition in LCMO materials [19]. Annealing results not only in the variation of oxygen stoichiometry, thus changing the distribution and number of Mn^{4+}-Mn^{3+} pairs, but it also enhances Mn replacement by Fe or Ni. In our opinion, similar effects on the alteration of pair distribution should be associated with significant structural difference between the investigated films and single-crystal substrates.

4. Conclusions

We have deposited epitaxial layers of Fe- or Ni-doped LCMO films on STO, LAO, and NGO substrates using the PLD technique, followed by post-annealing at 900 ^{o}C in oxygen atmosphere. SIMS analysis indicates that substantial amounts of Fe or Ni are incorporated into the films. Transition temperatures of 75 K and 220 K are obtained for films on different substrates. XAS and transport measurement suggests that the effect of the electronic structures on the physical properties of the LCMO films is related to the variation of the ratio of Mn^{4+} to Mn^{3+}.

Acknowledgments

The authors thank the assistance of Dr. F. Aduroduja for sample preparation and the staff of NSRRC during the experiments. This work is sponsored by the National Science Council, Taiwan, Republic of China under Grants Nos. NSC90-2112-M-018-006 and NSC 91-2811-M-018-001.

References

[1] S. Jin, T. H. Tiefel, M. McCromack, R. A. Fastnacht, R. Ramesh, L. H. Chen, Science **264**, 413 (1994).
[2] M. McCromack, S. Jin, T. H. Tiefel, R. M. Fleming, J. M. Phillips, R. Ramesh, Appl. Phys. Lett. **64**, 3045 (1994).
[3] J. Y. Gu, K. H. Kim, T. W. Noh, K. S. Suh, J. Appl. Phys. **78**, 6151 (1995).
[4] R. von Helmolt, J. Wecker, B. Holzapfel, L. Schultz, K. Samwer, Phys. Rev. Lett. **71**, 2331 (1993).
[5] H. S. Choi, W. S. Kim, B. C. Nam, N. H. Hur, Appl. Phys. Lett. **78**, 353 (2001).
[6] C. J. Liu, C. S. Sheu, M. S. Huang, Phys. Rev. B **61**, 14323 (2000).
[7] J. W. Feng, L. P. Hwang, Appl. Phys. Lett. **75**, 1592 (1999).
[8] C. S. Huang, I. N. Lin, J. Y. Lee, T. Y. Tseng, Jpn. J. Appl. Phys. **33**, 4058 (1994).
[9] M. H. Yeh, K. S. Liu, J. Appl. Phys. **77**, 5335 (1995).
[10] S. K. Hau, K. H. Wong, P. W. Chan, C. L. Choy, Appl. Phys. Lett. **66**, 245 (1995).
[11] S. Jin, M. McCromack, T. H. Tiefel, R. Ramesh, J. Appl. Phys. **76**, 6929 (1994).
[12] S. Y. Bae, S. X. Wang, Appl. Phys. Lett. **69**, 121 (1996).
[13] C. J. Liu, M. S. Huang, C. S. Sheu, Chin. J. Phys. **38**, 360 (2000).
[14] C. J. Liu, M. S. Huang, unpublished.
[15] S. W. Cheong, C. H. Chen, Colossal Magnetoresistance, Charge Ordering and Related Properties of Manganese Oxides, eds. C. N. R. Rao and B. Raveau, World Scientific, Singapore (1998).
[16] Y. Tomioka, A. Asamitsu, H. Kuwahara, Y. Moritomo, Y. Tokura, Phys. Rev. **B 53**, R1689 (1996).
[17] Y. Tomioka, A. Asamitsu, Y. Moritomo, H. Kuwahara, Y. Tokura, Phys. Rev. Lett **74**, 5108 (1995).
[18] P. G. Radaelli, D. E. Cox, M. Marezio, S. W. Cheong, Phys. Rev. B **55**, 3015 (1997).
[19] J.-S. Zhou, J. B. Goodenough, Phys. Rev. B **58**, R 579 (1998).